


# Spatial Optimization of Charging Networks for Heavy-Duty EVs Using Hexagonal Discrete Models

Germano B. dos Santos   [ Universidade Federal Viçosa/ Manna Team | [germano.santos@ufv.br](mailto:germano.santos@ufv.br) ]


Guilherme C. Melos  [ Universidade Federal de Viçosa | [guilherme.melos@ufv.br](mailto:guilherme.melos@ufv.br) ]

Leonardo J. A. S. Figueiredo  [ Universidade Federal de Minas Gerais | [leonardo.alves@dcc.ufmg.br](mailto:leonardo.alves@dcc.ufmg.br) ]

Fabício A. Silva  [ Universidade Federal de Viçosa/Manna Team | [fabicio.asilva@ufv.br](mailto:fabicio.asilva@ufv.br) ]

Thais R. M. B. Silva  [ Universidade Federal de Viçosa/Manna Team | [thais.braga@ufv.br](mailto:thais.braga@ufv.br) ]

Antonio A. F. Loureiro  [ Universidade Federal de Minas Gerais | [loureiro@dcc.ufmg.br](mailto:loureiro@dcc.ufmg.br) ]

 IEF, Universidade Federal de Viçosa - Campus Florestal, Rodovia LMG818, km6, Florestal-MG, 35690-000, Brazil

**Received:** 01 October 2024 • **Accepted:** 26 February 2025 • **Published:** 30 May 2025

**Abstract** Due to the environmental impact caused by greenhouse gas emissions, solving problems aimed at increasing the usage of electric vehicles became important. Personal Electric Vehicles are being highly adopted by society in order to reduce emissions. However, a prominent part of air pollution is provided by heavy-duty vehicles, such as trucks, and its electrification is challenging because of the lack of government policies and charging infrastructure. In light of this, electric charge stations should be located considering the truck drivers' route to increase its adoption. Therefore, this study proposes two hexagonal discrete covering models, a Hexagonal P-Median (HPMP) and Hexagonal Capacitated Location Set Covering (HCLSCP), enhancing the space complexity of classical discrete models to cover the Brazilian truck drivers' route. Furthermore, we compare the novel hexagonal models to a greedy method using a spatio-temporal simulation. We consider the infrastructure limitations with capacity constraints and waiting time in recharging queues with real-world data comprising locations of 3,086 drivers. The results show a trade-off between infrastructure cost, coverage demand, and queuing performance. The HPMP is ideal for covering demand, while the greedy method minimizes infrastructure cost, and HCLSCP outperforms the other models in queuing management.

**Keywords:** electric vehicles, charging station placement, facility-location, spatio-temporal simulation, real-world data

## 1 Introduction

The transport electrification is a key component of the world decarbonization process, impacting diverse economic sectors, including job creation and transforming supply chain operations [Tamba *et al.*, 2022]. Moreover, this process is advantageous for the environment due to zero or reduced greenhouse emissions. According to the Global EV Outlook 2024 [IEA, 2024], the adoption of heavy-duty electric vehicles (HDV), e.g., electric trucks, is increasing due to the expectation to reduce up to 92% of CO<sub>2</sub> emitted with the zero-carbon HDVs [O'Connell *et al.*, 2023]. Therefore, in collaboration with auto manufacturers, such as Volvo, Volkswagen, and Tesla, European and Emerging Market and Developing Economies are creating policies to foster the electrification process [Liimatainen *et al.*, 2019].

However, the HDV presents some limitations regarding refueling, such as long charging times, battery range, charging station infrastructure, and availability. These problems contribute to the 'range anxiety' — the driver's uncertainty about whether the battery will last for the intended travel distance. Such psychological effects are important in the decision to purchase an electric vehicle [Kchaou-Boujelben, 2021], and addressing these concerns is fundamental for the evolution of this market and future technological developments. Alongside this, the poor infrastructure can impact the shipping services as the charging station availability plays a critical role

in electrical vehicle route planning [Lin *et al.*, 2016] since the recharging time can delay the trip and increase the labor cost. Therefore, the success of HDV is correlated to the development of well-planned road and highway infrastructure to support the demand, which can be done in different ways, such as providing an efficient energy grid power to accelerate the recharging time and increasing the charging station availability.

The issue of long recharging time can be viewed as a multifaceted challenge. The energy grid of the country or city must be robust to supply the demand [Ahmad *et al.*, 2023]. Alternatively, battery swapping can be infeasible since the size of an HDV battery is larger than a personal electric vehicle, increasing operational costs [Deng *et al.*, 2023]. In light of this, hydrogen fuel cells are being developed to accelerate the recharging time. However, to support the hydrogen fuel, it is required to have a high-quality distribution network, necessitating significant government investments in infrastructure and fuel production [Gündüz *et al.*, 2024].

Hence, expanding the availability of charging stations necessitates careful planning, which can be achieved by analyzing results from discrete allocation models [Kchaou-Boujelben, 2021], that treat the demand as a discrete point in space, aiming to minimize the costs of a charging station ensuring all driver demand points are satisfied.

Zafar *et al.* [2021] model charging station placement problem by solving maximal coverage location of demand points

and Iravani [2022] performs charging station selection by partitioning a maximal coverage model using a spatial index. He *et al.* [2016] discuss that the P-Median model [Church *et al.*, 2018] has better results in comparison to maximal coverage models. However, these works ignore some restrictions that impose a more realistic modeling, such as considering grid distribution power, capacity constraint, and queue waiting times.

Therefore, in this work, we introduce a novel method to manage a large-scale area of study and a high volume of demand points through H3 partitioning, transforming the Capacitated Set Covering and P-Median into Hexagonal Capacitated Location Set Covering (HCLSCP) and Hexagonal P-Median (HPMP), respectively. This transformation reduces the asymptotic space complexity of the client-demand matrix, making the discrete models feasible for our study. Furthermore, we compare these models with a discrete greedy model [Lam *et al.*, 2014] to optimize the placement of charging stations based on 45 million records of Brazilian driver trajectories. This dataset comprises 180,000 demand points and 42,000 petrol stations in Brazil as potential sites. Additionally, we propose a time-based simulation over the charging stations sited, considering the capacity constraints, charging time, and queuing time.

This study also provides a quantitative comparison between the discrete model approaches using our novel time-based simulation metrics. The greedy model preserves the reachability of all sited charging stations, maintaining the graph connected with a minimal number of charging stations. HPMP minimizes the distance between a demand and a potential site, while the HCLSCP minimizes the number of facilities sited subject to the capacity constraint (i.e., how many drivers can recharge simultaneously).

In summary, our contributions can be listed as follows:

- A novel method to transform a discrete model to a hexagonal discrete model in order to reduce the asymptotic space complexity;
- A spatio-temporal simulation considering capacity constraints and queuing time;
- Novel simulation metrics, waiting queue, and recharging time, to evaluate the efficiency of discrete covering models in charging station placement problem;

This work is an extension of the paper published at the VIII Workshop de Computação Urbana (CoUrb 2024) [Santos *et al.*, 2024]. In this new version, we have introduced a novel method (i.e., HCLSCP) for spatial partitioning in discrete covering models, considered capacity limitations, and added a quantitative comparison between capacity-constrained and non-capacity-constrained models (e.g., HPMP and greedy). Moreover, we propose a time interpolation method and a spatio-temporal simulation to evaluate three metrics: total recharging time, queue waiting time, and infrastructure cost, in order to assess the models from a real-world data perspective.

The remainder of this work is organized as follows: Section 2 highlights the recent charging station models in the literature. Section 3 presents the formulation of classical discrete covering models. Section 4 discusses the novel

method to reduce the space complexity of the discrete covering model. The data used and the spatio-temporal simulation proposed are outlined in Section 5. Finally, the results and conclusion are presented in Section 6 and Section 7, respectively.

## 2 Related Work

A few studies that propose solutions to charging station placement consider only a city or a region as a study area, reducing complexity in terms of space [Iravani, 2022; Lam *et al.*, 2014; Zafar *et al.*, 2021]. Lam *et al.* [2014] modeled the problem as a graph connectivity problem, such that the vertices are gas stations in the study area and the edges are the shortest paths between the gas stations. Hence, a simulation, using Hong Kong as a region, is proposed to evaluate the model performance regarding the total cost and computation time. From another perspective, Zafar *et al.* [2021] define the charging station location-allocation as a Maximum Coverage Location Problem (MCLP) [Church *et al.*, 2018], considering the city of Raleigh, North Carolina.

Similarly, other works follow the strategy to supply the demand points with discrete models, albeit with various constraints. For instance, Iravani [2022] addresses the problem using MCLP optimization constrained by the population census attributes, with the model partitioned by a spatial index for Dubai. Moreover, Cui *et al.* [2019] focus on minimizing the overload energy grid network by adding a new charging station in Singapore. Although these constraints increase the realism of the solution, they are difficult to fulfill on a national level. Therefore, this present study employs a more flexible approach to assess the coverage of driver trajectories for siting charging stations. Consequently, the framework proposed can be explored in different scenarios within a countrywide context.

Additionally, other works have explored alternative optimization approaches. Xiong *et al.* [2017] propose a model based on game theory, assuming that drivers aim to minimize both recharging and queuing times. Human mobility patterns can also provide insights into the individual driver preferences for siting electric charging stations. For instance, Wu *et al.* [2024] define the population demand for recharge by considering the daily shifting (e.g., home-work, work-other), within California as a study area, allowing the rearrangement of trajectories based on the location of charging stations. In [Hu *et al.*, 2024], the demand of Ningbo, China, is analyzed using an autocorrelation perspective on origin-destination flows. Machado *et al.* [2020] prioritize neighborhoods in São Paulo, Brazil, by ranking the need for charging stations using a multivariate analysis based on travel frequency and points of interest. However, it is infeasible to conduct mobility and census data analysis at a national level, to locate the charging stations for heavy-duty electric vehicles, as this work addresses.

On the other hand, simulation-based approaches are widely employed to evaluate optimization models [Bi *et al.*, 2017; Xiong *et al.*, 2021] as this technique is efficient in approximating real-world behavior at a reduced computational cost [Viswanathan *et al.*, 2016]. For example, Andrade

*et al.* [2020] utilize a Monte Carlo simulation of highway traffic flow to assess the demand for electric stations in the metropolitan region of São Paulo. Similarly, Bi *et al.* [2017] introduce a multi-objective model in Singapore, designed to minimize the number of stations while maximizing their utilization through a simulation-based analysis. Moreover, Jahangir *et al.* [2022] simulate the electric vehicle demand characteristics (arrival and departure time, and voltage demand).

In contrast to these works, this study stands out by leveraging fine-grained real-world truck driver data, focusing on individual trajectories rather than generalized mobility patterns like origin-destination matrices. Furthermore, it is the first study, to the best of our knowledge, to compare a capacity-constrained discrete model with optimization techniques. While real-world trajectories are analyzed, this study also proposes a spatio-temporal simulation to ensure that all drivers can complete their routes with charging stations sited, considering the time waiting for queues and demand coverage.

### 3 Background and Preliminaries

In this section, the theory of classical discrete location covering models is presented through a lens of the charging station siting problem. These spatial optimization models share common characteristics: demand points and facility sites. In this work, we assume that the demand points are the locations where the heavy-duty vehicles run out of fuel, i.e., where they exceed their battery range, while the facilities sites are the petrol stations leveraging the pre-existing gas fuel infrastructure, and the highway network is a graph such that vertices are the highway junctions, where the demand points and facilities are located, and edges are the highways segments. The discrete models are classified based on how they relate demand points to facility points within the cost function. In this study, we enhance two classical models with the framework proposed in Section 4: the Location Set Covering Model (LSCP), which aims at minimizing the number of facilities required to ensure all demand points are covered within a radius defined by a maximal service distance or time [Church *et al.*, 2018], and the P-Median Model (PMP), which minimizes the total demand distance between each demand point and the nearest facilities.

Additionally, to approximate real-world conditions, constraints such as infrastructure limitations can be included, as outlined in Section 2. For example, a capacity constraint implies that the charging station can attend up to  $k$  truck drivers simultaneously, imposing a hard restriction on the discrete models. The following sections present the formulations of the LSCP and PMP models, considering these restrictions.

#### 3.1 Capacitated Location Set Covering (CLSCP)

The Location Set Covering model aims to minimize the number of the sited facilities to cover all the demand points without considering the capacity constraints, i.e., regarding the charging stations problem, the located stations will have an infinite number of recharging points. This model is widely

applied in such facility location problems [Santos *et al.*, 2024; He *et al.*, 2016] due to low computational cost. However, it does not account for the level of demand in each area, being out of reality in some optimization problems such as those discussed in this study. Then, differently from the previous discussions on locating recharging stations in the literature, we leverage the capacity constraint to impose real-world infrastructure limitations [Current and Storbeck, 1988]. The capacitated version of LSCP is formulated as follows:

$$\text{Minimize} \quad \sum_{j \in J} x_j \quad (1)$$

$$\text{Subject to:} \quad \sum_{j \in N_i} z_{ij} = 1 \quad \forall i \in I \quad (2)$$

$$\sum_{i \in I} a_i z_{ij} \leq C_j x_j \quad \forall j \in J \quad (3)$$

$$x_j \in \{0, 1\} \quad \forall j \in J \quad (4)$$

$$z_{ij} \geq 0 \quad \forall i \in I \quad \forall j \in N_i \quad (5)$$

**Where:**

$I$  = demand points

$J$  = set of stations

$S$  = maximum service radius

$d_{ij}$  = geographic distance between the demand  $i$  and station  $j$

$N_i = \{j \mid d_{ij} < S\}$

$a_i$  = demand level in  $i$

$C_j$  = capacity of the potential station  $j$

$x_j$  = binary decision variable that indicates if station  $j$  was selected

$z_{ij}$  = fraction of demand  $i$  that is allocated to station  $j$

Equation (1) is the coverage cost function as already explained. Equation (2) asserts that the sum of fraction demand  $i$  is equal to 1, meaning that 100% of demand should be covered by one or more facilities. Consequently, all allocations should be within a maximum service radius. Equation (3) asserts that the allocated demand to each facility  $j$  does not exceed its defined capacity,  $C_j$ . Note that if the station  $j$  does not be chosen to effectively site, then  $x_j = 0$  and the effective capacity on the right side of Equation (3) will be equal to zero. This will limit the sum of allocation to this station to zero, guaranteeing that the demand will be served only by selected stations. This model assigns the demand according to the system convenience [Church *et al.*, 2018] so that all demand served does not exceed the sum of selected station capacities. Constraint (4) asserts that the decision variables should be binary variables, while constraint (5) imposes non-negative constraints, that is, only positive and zero values should be assigned to decision variables.

#### 3.2 P-Median (PMP)

The P-Median model is different from LSCP when comparing the objective function. The PMP minimizes the weighted distance between the demand and a facility site with a maximum of  $p$  facilities. This facility constraint sets a specific characteristic to PMP, since it is challenging to assign the minimum value that minimizes the distance while serving the truck drivers' trajectories. Considering Equation (3) from the formulation of LSCP above, the PMP model would require more facilities with capacity  $k$  than the number of demand points for each demand area - thus increasing the fixed costs to our recharging station problem, since our demand points

are all the locations in a highway where the truck drivers run out of fuel (See Section 5.1). Consequently, the recharging station problem is modeled as a P-Median problem without capacity constraint.

$$\text{Minimize} \quad \sum_{i \in I} \sum_{j \in J} d_{ij} X_{ij} \quad (1)$$

$$\text{Subject to:} \quad \sum_{j \in J} X_{ij} = 1 \quad \forall i \in I \quad (2)$$

$$\sum_{j \in J} Y_j = p \quad (3)$$

$$X_{ij} \leq Y_j \quad \forall i \in I \quad \forall j \in J \quad (4)$$

$$X_{ij} \in \{0, 1\} \quad \forall i \in I \quad \forall j \in J \quad (5)$$

$$Y_j \in \{0, 1\} \quad \forall j \in J \quad (6)$$

**Where:**

$I$  = demand points

$J$  = set of stations

$p$  = quantity of stations should be located

$d_{ij}$  = geographic distance between the demand  $i$  and station  $j$

$$X_{ij} = \begin{cases} 1, & \text{if a station } j \text{ serve demand } i \\ 0, & \text{otherwise} \end{cases}$$

$$Y_j = \begin{cases} 1, & \text{if station is located on vertex } j \\ 0, & \text{otherwise} \end{cases}$$

Equation (1) is the cost function of the PMP model, where the goal is minimizing the total demand weighted between each demand and the nearest recharging station. Equation (2) requires that each demand  $i$  be assigned to a unique station. Equation (3) asserts that the sum of located recharging stations should be equals to  $p$ . Equation (4) asserts that each demand should be assigned to a station  $j$  if and only if the station was selected. Constraints (5) and (6) are the decision variables non-negative conditions.

## 4 Spatial Hexagonal Discrete Models

In this section, we present the proposed enhancements to the discrete models presented in Sections 3.1 and 3.2. Our method reduces the asymptotic space complexity of both CLSCP and PMP, making them feasible to address the national-level charging station placement problem.

### 4.1 Hexagonal Partitioning Discrete Model

The demand-facility distance matrix rules the space complexity of the discrete model, resulting in  $\mathcal{O}(|I||J|)$  function, where  $I$  is the set of demand points, and  $J$  defines the set of stations. Given that this study focuses on solving the charging station placement on a national-level, it is infeasible to conduct experiments with a high volume of data. Then we propose reducing this complexity by applying a spatial partitioning index based on Tobler's Law [Tobler, 1970], also known as the First Law of Geography: *everything is related to everything else, but near things are more related than distant things*.

A partitioning method divides the large space into small areas, creating a tessellation  $T$  which is defined as a closed subset  $D = s_1, s_2, \dots, s_n$ , where  $s_i$  is a divided space. Moreover, given that  $s'_i$  is interior of  $s_i$ , then  $s'_i \cap s'_j = \emptyset$  and  $\bigcup_{i=1}^n s_i = T$ . In this work, we apply the H3 hexagonal parti-

tioning<sup>1</sup> because this polygon format presents useful properties and arranges the space into equal regions. Note that the partitioning can be applied with different methods, such as grid-based or Hilbert Space-based, nevertheless; the different sizes of regions could impact the space complexity since some regions can have many demand points while others can have a few points. Therefore, we enhance the discrete models (CLSCP and PMP) with H3 spatial partitioning, reducing the demand area for each hexagon produced by this processing.

The formulation of CLSCP is transformed to  $n$  instances, where each instance is a CLSCP model represented by equation 1, such that  $I_m$  is the demand points set from the  $m$ -th region,  $J_m$  is the facility locations from the  $m$ -th region, and  $C_m$  is a vector representing the capacities of each facility location in  $J_m$ . This novel model is named as Hexagonal Capacitated Location Set Covering Model (HCLSCP) aiming at minimizing the number of sited locations while covering all demand in minor areas, producing a solution set by union of small instances of CLSCP.

$$\text{HCLSCP} = \bigcup_{m=1}^N \text{CLSCP}(I_m, J_m, C_m) \quad (1)$$

Hence, the transformation of PMP works similarly, with  $n$  partitioned regions. The optimization function is defined as Equation 2, so that  $I_m$  is the demand points set from the  $m$ -th region,  $J_m$  is the facility locations from the  $m$ -th region and  $p_m$  is the number of desired facilities in the region  $m$ . For each region, the function P-Median minimizes the distance between the recharging points  $J_m$  and the demand points  $I_m$  in the hexagonal region  $m$ . Therefore, the solution set is the union of each PMP hexagonal model; thus this hexagonal discrete model is named as Hexagonal P-Median (HPMP).

$$\text{HPMP} = \bigcup_{m=1}^N \text{P-Median}(I_m, J_m, p_m) \quad (2)$$

### 4.2 Baseline

The greedy solution presented in Lam *et al.* [2014] is implemented to compare the classical hexagonal discrete models since it is a method that adheres to our high-volume data compared to the other models. Then, in our comparison, we have three discrete models: two that account for capacity (Greedy and HCLSCP) and one (HPMP) that does not consider it.

The formulation of [Lam *et al.*, 2014] utilizes a graph  $G(P, C)$  composed of vertices  $P$  and edges  $C$  representing the stations and a path  $c_d$  between the station  $p_i$  and  $p_j$ , respectively. Given  $p_i, p_j$  and the  $c_d = \text{Dijkstra}(p_i, p_j)$ ,  $c_d$  should be less than the maximum distance of battery range, defined as an input parameter. Hence, the model aims to minimize the total cost so that the demand of each highway is represented by the driver flow rate being served.

The greedy strategy proposed by [Lam *et al.*, 2014] is defined by removing a vertex of graph  $G$ , such that the demand could be served yet and the number of connected components  $\omega_G$  remains equal to 1. In [Lam *et al.*, 2014], it is calculated

<sup>1</sup><https://h3geo.org/>

in each iteration the set of vertices  $\bar{P}$  that could be removed. Hence, it is possible to refine this algorithm complexity, since the set can be calculated once, reducing the complexity from  $\mathcal{O}(\bar{P}(|C| + |P| + |R|))$  to  $\mathcal{O}((|C| + |P|) + |\bar{P}||R|)$ . This enhancement is important to our study, as  $|\bar{P}|$  is large.

## 5 Data and Simulation

In this section, we discuss how we interpolate the drivers' locations data and our simulation algorithm with their metrics, considering the stations allocated by the algorithms in Sections 3.1, 3.2, and 4.

In this work, we utilize real-world data comprising 3,086 Brazilian truck drivers for the experiments. A mobile application tracked the locations periodically for each driver, thus enabling the estimation of their trajectories. This dataset, collected from 03-28-2021 to 06-10-2021, was provided by a partner company under a confidentiality agreement.

It is important to highlight that data collection occurs intermittently, as it would not be feasible for the driver to have the application tracking GPS location data continuously. A data interpolation method is proposed (See Section 5.2) to minimize the impact of these intervals imposed by real-world data conditions.

### 5.1 Data Characterization

Let a record be denoted by  $l_i = \langle \text{latitude}, \text{longitude}, \text{timestamp}, \text{error} \rangle$ , such that latitude and longitude correspond to geographic coordinates, timestamp the time when the record was tracked. The error represents the precision of the point, in meters.

Considering that the data presents a real-world context, the records may be spurious. To maintain the data consistency, a filtering process was applied. Let  $L$  represent the set of records for all drivers, and  $L_u$  be the sequence of records for a particular driver  $u$ . The variable  $\text{timestamp}_{u,i}$  denotes the  $i$ -th *timestamp* for the driver  $u$ . We define  $\Gamma_u$  as the average number of records per day for driver  $u$ , where  $\Gamma_u = |L_u| / \text{days}(\max(\text{timestamp}_{u,i}) - \min(\text{timestamp}_{u,i}))$ . Thus, drivers that satisfy  $\Gamma_u < 1$  were excluded to prevent skewing the results. Additionally, records where the *error* is greater than 2 km, representing 20% of the dataset entries, were also removed. This distance (2 km) was chosen since it is considered the minimum necessary to accurately map a charging station to a location record. These filters resulted in a database with 3,086 drivers, with approximately 2.5 million points.

Analyzing the individual measures, such as mean travel distance per day and mean travel speed, is important to characterize the behavior of each truck driver [Akter and Hernandez, 2023]. Regarding Figure 1 it is notable that most drivers travel less than 300 km per day, which is comparable to the [Liimatainen *et al.*, 2019] study. Alongside this, Figure 2 reveals a similar median travel speed compared to [Lin *et al.*, 2016], 40 km/h.

In addition to the data collected by mobile devices, a public database from the ANP (*Agência Nacional do Petróleo*,

*Gás Natural e Biocombustíveis do Brasil*) was used, containing 42,000 station coordinates across Brazil<sup>2</sup>. In this work, gas stations are candidates to become electrical charging points, to contribute to the infrastructure.

### 5.2 Data Interpolation

As described above, the data used is real and the collection of consecutive records is done at pre-defined intervals, i.e., the location tracking  $l_{u,i+1}$  is performed at  $t_{u,i+1}$  where  $t_{u,i}$  is the timestamp related to the point  $l_{u,i}$ . Hence, the route may be discontinuous since the driver's trajectory could be represented by road segments rather than the entire highway. The data interpolation method proposed is divided into two steps, a spatial interpolation supported by Dijkstra's algorithm and a time interpolation based on the individual driver's average travel speed. The spatial and time-based interpolation is essential for the simulation proposed, since the route trajectories are completed regarding the trajectories within a time span.

Firstly, the road segment of a data point was identified by using a combined solution of *OpenStreetMap*<sup>3</sup> (OSM) repository, to obtain the highways in Brazil along with spatial indexes. Let the highway network be represented as a graph  $H(V, R)$ , such that  $R$  is the edges set and  $V$  the vertices, representing the highway segments and junctions, respectively. Each point  $l_{u,i}$  was then indexed to an edge  $r_j$  using the *BallTree* spatial index [Omohundro, 1989] to find the closest highway segment given the geographic distance. The edge  $r_j$  is represented by  $\text{geom}_{r_j}$  in the point's definition. Moreover, the vertices identifiers associated with  $R$ ,  $v_1^{r_j}$  and  $v_2^{r_j}$ , are also included in the point's definition. Consequently, the enriched record is defined as  $l'_{u,i} = \langle \text{latitude}, \text{longitude}, \text{geom}_{r_j}, v_1^{r_j}, v_2^{r_j}, \text{timestamp} \rangle$ . Here, the value *error* is disregarded as the filter processing has already been done. For the remainder of the work, this enriched record will be used as the data point.

Regarding the discontinuous trajectories, it is necessary to complete the data such that the preceding road segment  $r_{u,j}$  is immediately adjacent of  $r_{u,j+1}$ . To this end, each driver's point was ordered according to *timestamp*, resulting in an enriched record list  $L'_u$ . Thus, Dijkstra's algorithm

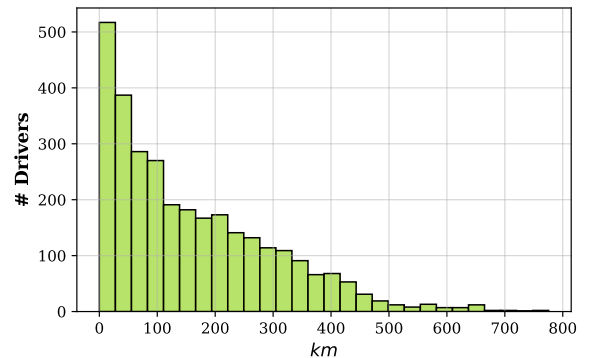


Figure 1. Mean Travel Distance Per Day

<sup>2</sup><https://www.gov.br/anp/pt-br/centrais-de-conteudo/dados-abertos/dados-cadastrais-dos-revendedores-varejistas-de-combustiveis-automotivos>

<sup>3</sup><https://www.geofabrik.de/>



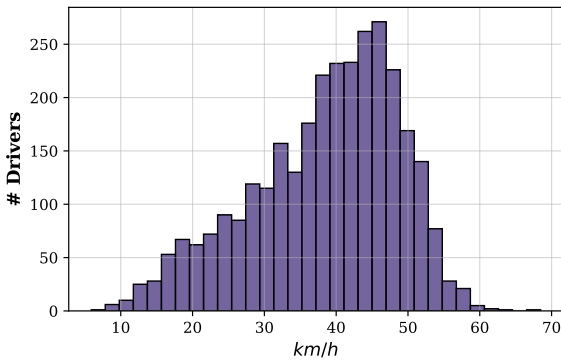


Figure 2. Mean Travel Speed

[Dijkstra, 1959] was used to identify the shortest path based on the graph  $H(V, R)$ , using the length of the road segment in meters as the weight of the edge. This created interpolated points between the enriched records  $l'_{u,i}$  and  $l'_{u,i+1}$ ,  $\{l'_{u,i}, l'_{u,i+1}\} \in L'_u$ . This method added 43 million interpolated points, resulting in a dataset composed of 45.5 million locations. It is important to note that Dijkstra's Algorithm operates between one location and the subsequent one, rather than between the points of origin and destination; therefore, the shortest path assumed to be the actual route is likely to be followed by the driver.

Figure 3 represents the spatial interpolation method proposed, where the left side is the trajectory incomplete with 2,161 points and the right side represents the complete trajectory after the interpolation processing, with 41,795 location points.

In the second step, the time-based interpolation follows the average travel speed defined by Equation 3.

$$\mu_u = \frac{\sum_{i=1}^{|L'_u|} d(l'_{u,i}, l'_{u,i-1})}{\max(L'_u(\text{timestamp})) - \min(L'_u(\text{timestamp}))} \quad (3)$$

The  $d(l'_{u,i}, l'_{u,i-1})$  is the distance of subsequent locations of the driver's route. Consequently, the time interpolation can be defined as  $\text{timestamp}_{u,i+1} = d(l'_{u,i}, l'_{u,i+1})/\mu_u + \text{timestamp}_{u,i}$  and is applied sequentially to all records for the user, up to the last location. Note that is required the driver to have the first record with a timestamp, and the following one is replaced by the average speed interpolation process.

It is important to note that there are other sophisticated methods to fill gaps in trajectories [Chen *et al.*, 2023; Celes *et al.*, 2017]. However, they are computationally complex since they consider different contexts and information. Thus, we decided to use the interpolation method, which satisfactorily addresses our expectations.

### 5.3 Spatio-temporal Simulation

The simulation methods presented in [Bi *et al.*, 2017] estimate the trip consumption based on the mechanical motor modeling considering the airflow, rolling, and inertia. However, the authors do not account for infrastructure limitations; if the electric vehicle needs to recharge, it is assumed to be able to do so, regardless of how many recharging points are available at the station. This aspect is frequently overlooked

in the literature. Similarly, Santos *et al.* [2024] also implies that exist an infinite number of stations capable of simultaneously recharging any electric vehicle. In light of this, we propose a spatio-temporal simulation that accounts for recharging time and station capacity, incorporating the infrastructure limitations into the simulation model.

The spatio-temporal simulation is anchored in two types of charging station usage behaviors, described by Bi *et al.* [2017]: 1) necessary recharging; 2) convenience recharging. The former refers to situations where the recharging is essential as the travel cannot be completed with the current battery level, while the latter represents the scenario where the driver recharges without significant detours even though can finish their route. In this work, we assume that the driver decides independently when to recharge, meaning that the stops are not previously planned. Furthermore, it is assumed that the truck drivers would like to maximize battery usage, minimizing the number of stops and detours when possible. Hence, the algorithm incorporates these restrictions in order to compare the influence of a capacity-constrained model with two discrete models under a resource-constrained infrastructure situation. The spatio-temporal simulation has two inputs, the ordered points set  $L$  and the enriched records  $L'$ . In the context of necessary recharging, the algorithm initializes a queue for a charging station when the number of drivers recharging concurrently exceeds its capacity, resulting in increased waiting times and subsequent shifts in the timestamps of the routes. This queue is a heap priority queue, a data structure that dequeues the first driver at the front, guaranteeing that the records remain ordered.

Table 1. Notations.

Notation	Meaning
<b>Set and subscripts</b>	
$u$	Driver
$L$	Ordered records
$L'$	Ordered enriched records
$P$	Recharging stations
<b>Input Parameters</b>	
$\alpha'$	Battery range
$\zeta_1, \zeta_2$	Detour limits
<b>Decision Variables</b>	
$p$	Best reachable station identified
$i$	Current location of the driver
$j$	Position on the subsequence $L'_u$
$\alpha$	Remaining battery level

Algorithm 1 adopted a greedy approach aimed at minimizing the number of stops to recharging as long as maximizing the battery range as well. This is supported by the procedure *NextReachableRechargingStation*, which identifies the furthest recharging point for the current location considering the truck driver's existing battery level. By prioritizing the most distant recharging station points, the algorithm enhances efficiency and extends the vehicle's travel distance before the next recharge. Furthermore, the proposed algorithm employs the constant  $\zeta$  to minimize the required detour for recharging

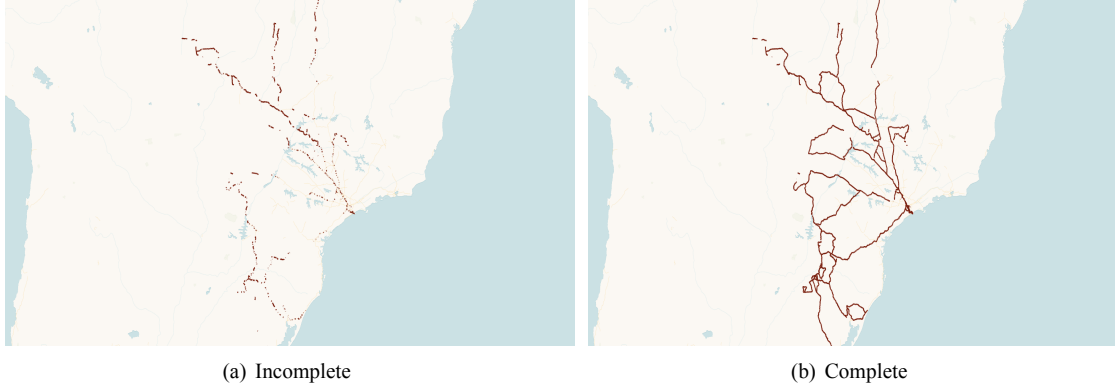


Figure 3. Truck Driver's Spatial Trajectory Interpolation

**Algorithm 1** Spatio-Temporal Simulation

```

1: procedure NextReachableRechargingStation
2:   Input:  $L'_u, \alpha', \zeta_1, \zeta_2$ 
3:    $m \leftarrow 0$   $\triangleright$  Furthest recharging station index
4:    $n \leftarrow +\infty$   $\triangleright$  Lowest detour found
5:    $D \leftarrow 0$   $\triangleright$  Distance traveled to recharging.
6:   for  $l'_{u,i} \in L'_u$  do
7:      $d \leftarrow \text{geographicDistanceClosestStation}(l'_{u,i})$ 
8:     if  $d < \zeta_1$  and  $\alpha' \geq D + d$  then
9:        $m \leftarrow i$ 
10:    elseif ( $m = 0$ ) and ( $d \leq n$ ) and ( $d < \zeta_2$ ) and
      ( $\alpha' \geq D + d$ ) then
11:       $m \leftarrow i$ 
12:       $n \leftarrow D$ 
13:       $D \leftarrow D + \delta(l'_{u,0}, l'_{u,i})$ 
14:   return ( $d, m$ )  $\triangleright$  Chosen recharging station.
15:
16: procedure  $\sigma$ 
17:   Input:  $L_u, L'_u, i$ 
18:    $j, p \leftarrow \text{NextReachableRechargingStation}(L'_u)$ 
19:   if  $i == j$  then
20:     if  $\text{CanRecharge}(p)$  then  $\text{Recharge}(u, p)$ 
21:     else  $\text{Enqueue}(u, p)$ 
22:    $\alpha \leftarrow \alpha - \delta(l'_{u,i-1}, l'_{u,i})$ 
23:   if  $\alpha \geq 0$  then
24:     return True  $\triangleright$  The driver  $u$  can reach at record  $i$ 
25:   return False

```

while allowing the truck driver to decide to reroute within a large radius. If no station is located within a geographic distance less than  $\zeta_1$ , the limit  $\zeta_2$  is used as a maximum threshold to select the station, such that  $\zeta_2 > \zeta_1$ . For this, in the loop (line 6), it tries to find the furthest possible station that the battery is sufficient to reach by applying the BallTree algorithm (line 7). In the case of no station is found, the station with the slightest deviation is chosen as long as the deviation is smaller than the limits. Finally, returning to the chosen station with distance and next point index.

The procedure  $\sigma$  optimizes the decision-making process. In line 18, an advancement is made to the next reachable recharging station indicated by  $m$ . Hence, it is unnecessary to repeat the *NextReachableRechargingStation* procedure to the location  $L_{u,(i+1)}$  adjacent to  $L_{u,i}$  if there is a station close to  $L_{u,(i+w)}$ , where  $w \geq i$  is set to be visited.

**Algorithm 2** Procedure  $\Sigma$ 

```

1: procedure  $\Sigma$ 
2:   Input:  $L, L', P$ 
3:    $fp \leftarrow \text{InitHeapPriorityQueue}(L)$ 
4:   do
5:     if ( $\text{timestamp}_i + \text{DriverDelay}(u) >$ 
       $\text{updatedtimestamp}_i$ ) then
6:        $fp \leftarrow \text{RemoveAtFront}(fp)$ 
7:        $\text{updatedtimestamp}_i \leftarrow (\text{timestamp}_i +$ 
       $\text{DriverDelay}(u))$ 
8:        $fp \leftarrow \text{AddRecordInQueue}(fp, P_i)$ 
9:     else  $\sigma(L_u, L'_u, i)$ 
10:   while  $|fp| > 0$ 

```

Algorithm 2 is responsible for maintaining the locations ordered to be iterated by the priority queue. When a truck driver has a low battery level, the *timestamp* should be updated such that the recharging time influences on the shift the next location times. In this spatio-temporal simulation, it is considered the recharging times and the waiting time in queues.

During the simulation, the driver  $u \in M$  follows the trajectory  $L'_u$  ordered by the time of each location  $l'_{u,i} \in L'_u$ ,  $1 \leq i \leq |L'_u|$ . The driver has a battery range ( $\alpha$ ), which indicates the distance the driver can travel with the current battery level. In this work, we assume that  $\alpha \leq 300\text{km}$ , represents the average autonomy of a heavy-duty electric vehicle, following Liimatainen *et al.* [2019]. Furthermore, let  $\delta$  a function which defines the distance between two locations, such that  $\delta : L'_u \times L'_u \rightarrow \mathbb{R}$ :  $\delta(l'_{u,i}, l'_{u,j}) = \sum_{i=1}^{j-1} \delta(l'_{u,i}, l'_{u,(i+1)})$  is the distance traveled by the driver  $u$  on a highway considering the locations  $l'_{u,i} \in l'_{u,(i+1)}$ ,  $i \geq 1$ , then battery range is updated as follows:  $l'_{u,i}$ :  $\alpha = \alpha - \delta(l'_{u,i}, l'_{u,j})$ . Based on the calculated distance from function  $\delta$ , the algorithm checks if the current battery level of driver  $u$  is sufficient to reach the next location  $j$  from location  $i$ , determining whether driver  $u$  can continue the trajectory.

**5.3.1 Simulation Metrics**

Let  $\gamma : M \times P \rightarrow \{0, 1\}$  be the function that evaluates the coverage, indicating if a driver  $u \in M$  can complete his/her trajectory considering the recharging stations sited  $P$ ,

considering the discrete models. Therefore the total coverage of each model is defined by  $\sum_{u \in M} \gamma(L'_u, P)$ .

As mentioned in section 3, for each deployed station we have a cost  $C$ , which aims to be minimized. Assuming a unique cost  $w$  for each recharging station deployed, the total cost is defined as  $C = |P| \cdot w$ .

Additionally, to account for capacity limitations, the waiting times in queues is also considered. Suppose a driver arrives at the charging station at time  $t_a$ . If the driver gets queued, then it only starts recharging at time  $t_s$  and ends the process at time  $t_e$ . Therefore, there are three different waiting times: the waiting time while the driver is queued ( $t_s - t_a$ ), the waiting time while the driver is recharging ( $t_e - t_s$ ) and the total waiting time ( $t_e - t_a$ ), also denominated by arrival-to-end (A2E). So the percentage of in queuing waiting time from A2E for this driver is obtained by the Equation 4.

$$A2E = \frac{t_s - t_a}{t_e - t_a} \quad (4)$$

## 6 Experiments and Results

In this section, we show the experimental environment and the parameters of the three discrete models in Sections 3 and 4 using the simulation of Section 5.3. In other words, according to the charging stations allocated by each algorithm, we apply the simulator to analyze the quality of the chosen coverage. Moreover, the quantitative comparison between the models is discussed based on the demand coverage, waiting time in queues, and average time recharging. Also, a point distribution of each solution is shown to demonstrate how different the locations sited are with respect to the constraints considered in coverage modeling.

The models HCLSCP and HPMP were developed using the library *spopt* [Feng *et al.*, 2022], and the greedy approach was developed with the library *NetworkX*. The experiments were conducted on a cluster with the following specifications: 2 processors AMD Opteron 6376 (16 MB cache, 2.3 GHz, 32 cores) with 512 GB RAM. It is important to note that we created our simulation due to the size of the country and the extensive period of drivers' data. This choice is due to the lack of traffic data that considers these two features of our study.

The parameters for execution of the HCLSCP, HPMP, and the spatio-temporal simulation were varied to compare the impact of different configurations on the performance of each model. We assume that the battery range is equal to 300km following [Liimatainen *et al.*, 2019]. Hence, for hexagonal covering models, the resolution of  $H3^4$  was 5, which means that there are 2,016,842 hexagons and 12 pentagons in the grid. Therefore, this configuration defines an area less than the battery range defined. Specifically for HCLSCP, we solve the charging station problem for 5 different capacity levels  $C_j = \{1, 2, 3, 4, 5\}$ . Besides that, all stations have an equal capacity, independent if an area that has a higher demand. For HPMP, we assign  $p$  equals to 1, then the hexagonal region will have only 1 recharging station to

attend to all demand. Although the HPMP and Greedy do not have the capacity input parameter, we simulate the capacity for the selected charging station for all models discussed in this study, assuming that the capacity is equal in all stations. Moreover, the spatio-temporal simulation assumes that the recharging time is equal to 5 hours [Giuliano *et al.*, 2021].

The behavior of the three models under capacity constraints is illustrated in Table 1. While the HPMP and Greedy models do not inherently account for capacity constraints, the simulation incorporates a proxy to represent the total number of drivers that can recharge simultaneously. As a result, the number of selected charging stations remains constant for both Greedy and HPMP models, as they do not adjust based on capacity limitations.

Model	Capacity	# Charging Stations	% Coverage
HCLSCP	1	8,594	14.04
HCLSCP	2	10,182	24.68
HCLSCP	3	10,807	31.85
HCLSCP	4	10,224	36.87
HCLSCP	5	10,156	39.69
HPMP	-	4,002	87.99
Greedy	-	1,624	30.46

**Table 2.** Summary of each model regarding the amount of selected charging stations and coverage

The HCLSCP model reaches a plateau at a capacity of 3, selecting 10,807 charging stations. Beyond this point, the number of selected stations decreases as higher capacity allows each station to serve more demand. In contrast, the Greedy solution results in the fewest selected stations, with 1,624, followed by the HPMP model with 4,002 stations.

As capacity increases, the percentage of covered drivers improves for the HCLSCP model. Initially, it starts with a coverage of 14.04%, but surpasses the Greedy solution at capacity 3. This suggests that selecting fewer charging stations, as in the Greedy approach, is insufficient to meet the demand. In contrast, HCLSCP optimally distributes charging stations to effectively satisfy the capacity constraints, demonstrating its ability to handle increasing demand more efficiently as capacity grows. Thus, as shown in Figure 5, HCLSCP has a more efficient queuing time, demonstrating reduced waiting times for drivers and an enhanced recharging experience in comparison to other proposed models.

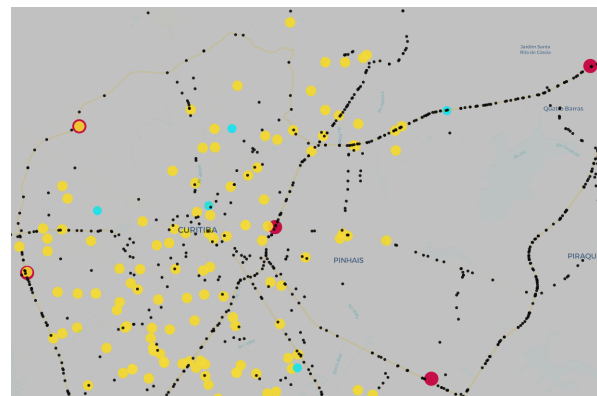


**Figure 4.** Selected charging stations of HCLSCP with capacity 5 (yellow), HPMP (red), and Greedy (cyan). Demand points are in black.

<sup>4</sup><https://h3geo.org/docs/core-library/restable/>



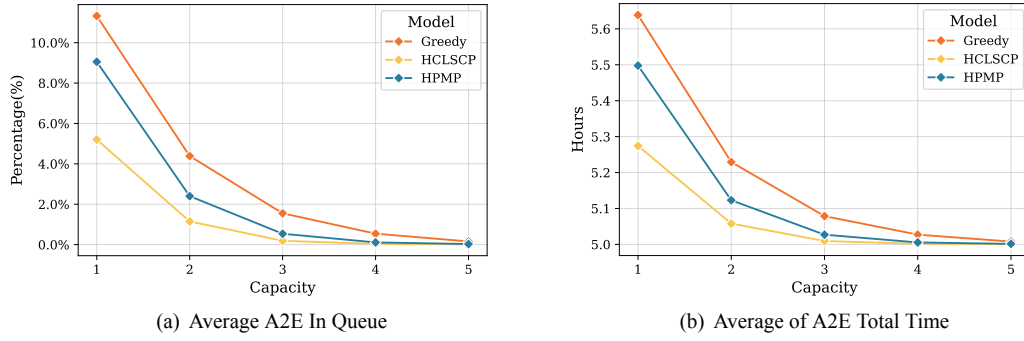


Figure 5. Arrival to End Waiting Times (A2E)

Once HCLSCP optimizes by capacity targets, it is observed that charging points are more concentrated towards regions where demand is dense, as shown in Figure 4 for the region of Curitiba, Paraná. This behavior happens because HCLSCP constraints allow a charging station to supply only a demand point. In contrast, HPMP minimizes the distance between a demand point and a facility. Hence, there are fewer selected charging stations in HPMP, due to the lack of capacity constraints, and those are distributed evenly across the hexagonal grid.

Additionally, without considering capacity constraints, such as HPMP and Greedy models, there is an increased waiting time to drivers, once there are fewer charging points to recharge the battery. This reduced availability of charging stations implied in more demand being sited at the same facility and therefore drivers had to wait more to recharge. Figure 5 highlights that on average HCLSCP reduces arrival to end waiting time (A2E) and also reduces the percentage in queue of A2E by 63.30% when compared to the Greedy model and by 45.69% when compared to HPMP model.

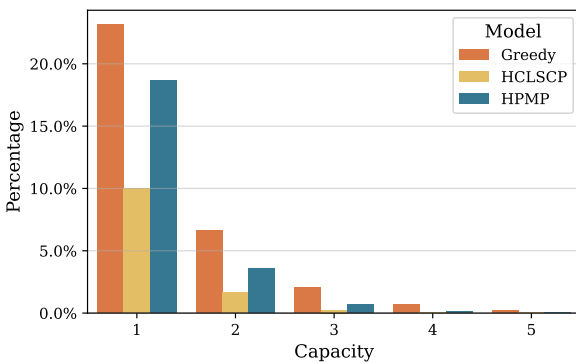


Figure 6. Percentage of queued recharges per capacity

As observed in Figure 5, for all models, the total queuing time decreases as capacity increases. Notably, the HCLSCP model outperforms the others in terms of both absolute queuing times and the total number of recharges that were queued. However, while increasing capacity reduces queuing times, it may also result in some recharging stations becoming underutilized, as the demand is more widely distributed across the network.

Finally, in Figure 6 it is possible to observe that, for capacity 1, 10% of all recharges in HCLSCP are queued.

This is the best minima across other models because HPMP performs with 18.67% and Greedy with 23.14%. Besides that, on average HCLSCP outperforms HPMP on average by 48.31% and outperforms Greedy by 63.40% on average of percentage of recharges queued, representing a reduced time spent for the drivers and a reduced of percentage of recharges that are queued.

## 7 Discussion and Future Works

This study evaluated the performance of three models — HCLSCP, HPMP, and a Greedy approach — for optimizing the placement of heavy-duty electric vehicle charging stations under varying demand and capacity constraints. The results highlight important trade-offs between the models in terms of coverage, infrastructure cost, and queuing performance.

The results indicate that the HCLSCP model consistently outperformed the others in key metrics such as waiting times and queue management. Meanwhile, Greedy is the most cost-effective and HPMP is the best in covering drivers' trajectories.

The HCLSCP model, which incorporates capacity constraints, demonstrated superior performance in efficiency. As capacity increased, the model optimized the distribution of charging stations, particularly in areas with higher demand density. The model reached a coverage plateau at capacity 3, selecting 10,807 charging stations and achieving a 31.85% demand coverage, which continued to improve as capacity grew. In contrast, the HPMP and Greedy models, which do not account for capacity constraints, performed worse in efficiency resulting in longer queuing times for drivers.

Additionally, HCLSCP showed a balanced performance. It did not achieve the highest coverage (max 39.69%) nor the lowest infrastructure cost, but it excelled in managing queuing times. HCLSCP significantly reduced the percentage of queued recharges by 63.40% compared to Greedy and by 48.31% compared to HPMP. As capacity increased, it optimized the placement of charging stations, distributing them more effectively in high-demand areas, and thus providing a more efficient recharging experience.

The HPMP model demonstrated the highest coverage, achieving 87.99%, despite selecting fewer charging stations compared to the HCLSCP model. This highlights the

model's efficiency in minimizing the distance between demand points and stations. However, due to its lack of capacity constraints, HPMP suffered from longer queuing times as fewer stations were available to meet the high demand in certain regions.

The Greedy model, while selecting the fewest charging stations (1624), thus minimizing the cost of infrastructure, had significantly lower coverage (30.46%) and the longest waiting times. This suggests that while the model is cost-effective in terms of station installation, it is not sufficient to meet high demand, resulting in increased queuing times and inefficiencies for drivers.

The queuing analysis highlighted that the HCLSCP model reduced arrival-to-end (A2E) waiting times by 63.30% compared to the Greedy model and by 45.69% compared to HPMP. Additionally, the percentage of recharges queued was significantly lower for HCLSCP, with a 48.31% improvement over HPMP and a 63.40% improvement over the Greedy model. These results underscore the advantage of considering capacity constraints and demand distribution when planning charging station networks.

Overall, these trade-offs highlight the strengths and limitations of each model. HPMP is ideal for maximizing coverage, Greedy minimizes infrastructure cost, and HCLSCP offers the best balance for managing capacity constraints and reducing queuing times.

Besides evaluating the trade-offs, it is important to highlight the differences between the models under comparable scenarios, thereby highlighting differences within coverage, cost, and service quality. Additionally, it is promising to combine two optimization strategies, leading to multiobjective framework to address multiple concerns around HDV. By exploring these future directions, it is expected that more robust and practical solutions will emerge to support the growing demand for heavy-duty EVs.

## Acknowledgements

The authors are thankful for the support of Capes, Softex, CNPq (Number 421548/2022-3) and Fapemig.

## Declarations

## Authors' Contributions

All authors contributed to the writing of this article, read and approved the final manuscript.

## Competing interests

The authors declare that they have no competing interests.

## Availability of data and materials

The datasets are private and are not available.

## References

Ahmad, F., Iqbal, A., Asharf, I., Marzband, M., and Khan, I. (2023). Placement and capacity of ev charging stations

by considering uncertainties with energy management strategies. *IEEE Transactions on Industry Applications*, 59(3):3865–3874. DOI: 10.1109/TIA.2023.3253817.

Akter, T. and Hernandez, S. (2023). Representative truck activity patterns from anonymous mobile sensor data. *International Journal of Transportation Science and Technology*, 12(2):492–504. DOI: 10.1016/j.ijtst.2022.05.002.

Andrade, J., Ochoa, L. F., and Freitas, W. (2020). Regional-scale allocation of fast charging stations: travel times and distribution system reinforcements. *IET Generation, Transmission & Distribution*, 14(19):4225–4233. DOI: 10.1049/iet-gtd.2019.1786.

Bi, R., Xiao, J., Pelzer, D., Ciechanowicz, D., Eckhoff, D., and Knoll, A. (2017). A simulation-based heuristic for city-scale electric vehicle charging station placement. In *2017 IEEE 20th International Conference on Intelligent Transportation Systems (ITSC)*, pages 1–7. DOI: 10.1109/ITSC.2017.8317680.

Celes, C., Silva, F. A., Boukerche, A., de Castro Andrade, R. M., and Loureiro, A. A. (2017). Improving vanet simulation with calibrated vehicular mobility traces. *IEEE Transactions on Mobile Computing*, 16(12):3376–3389. DOI: 10.1109/TMC.2017.2690636.

Chen, Y., Zhang, H., Sun, W., and Zheng, B. (2023). Rn-trajrec: Road network enhanced trajectory recovery with spatial-temporal transformer. In *2023 IEEE 39th International Conference on Data Engineering (ICDE)*, pages 829–842. IEEE. DOI: 10.1109/ICDE55515.2023.00069.

Church, R. L., Murray, A., et al. (2018). Location covering models. *Advances in Spatial Science*. DOI: 10.1007/978-3-319-99846-6.

Cui, Q., Weng, Y., and Tan, C.-W. (2019). Electric vehicle charging station placement method for urban areas. *IEEE Transactions on Smart Grid*, 10(6):6552–6565. DOI: 10.1109/TSG.2019.2907262.

Current, J. R. and Storbeck, J. E. (1988). Capacitated covering models. *Environment and planning B: planning and Design*, 15(2):153–163. DOI: 10.1068/b150153.

Deng, Y., Chen, Z., Yan, P., and Zhong, R. (2023). Battery swapping and management system design for electric trucks considering battery degradation. *Transportation Research Part D: Transport and Environment*, 122:103860. DOI: 10.1016/j.trd.2023.103860.

Dijkstra, E. W. (1959). A note on two problems in connexion with graphs. *Numerische mathematik*, 1(1):269–271. DOI: 10.1145/3544585.3544600.

Feng, X., Barcelos, G., Gaboardi, J. D., Knaap, E., Wei, R., Wolf, L. J., Zhao, Q., and Rey, S. J. (2022). spopt: a python package for solving spatial optimization problems in pysal. *Journal of Open Source Software*, 7(74). DOI: 10.21105/joss.03330.

Giuliano, G., Dessouky, M., Dexter, S., Fang, J., Hu, S., and Miller, M. (2021). Heavy-duty trucks: The challenge of getting to zero. *Transportation Research Part D: Transport and Environment*, 93:102742. DOI: 10.1016/j.trd.2021.102742.

Gündüz, S. B., Geçici, E., and Güler, M. G. (2024). Locating hydrogen fuel stations: A comparative study for istanbul. *International Journal of Hydrogen Energy*, 52:1234–1246.

- DOI: 10.1016/j.ijhydene.2023.10.295.
- He, S. Y., Kuo, Y.-H., and Wu, D. (2016). Incorporating institutional and spatial factors in the selection of the optimal locations of public electric vehicle charging facilities: A case study of beijing, china. *Transportation Research Part C: Emerging Technologies*, 67:131–148. DOI: 10.1016/j.trc.2016.02.003.
- Hu, X., Lei, H., Deng, D., Bi, Y., Zhao, J., and Wang, R. (2024). A two-stage approach to siting electric bus charging stations considering future-current demand. *Journal of Cleaner Production*, 434:139962. DOI: 10.1016/j.jclepro.2023.139962.
- IEA (2024). Global ev outlook. Technical report, IEA. Available at: <https://iea.blob.core.windows.net/assets/a9e3544b-0b12-4e15-b407-65f5c8ce1b5f/GlobaleVOutlook2024.pdf>.
- Iravani, H. (2022). A multicriteria gis-based decision-making approach for locating electric vehicle charging stations. *Transportation Engineering*, 9:100135. DOI: 10.1016/j.treng.2022.100135.
- Jahangir, H., Gougheri, S. S., Vatandoust, B., Golkar, M. A., Golkar, M. A., Ahmadian, A., and Hajizadeh, A. (2022). A novel cross-case electric vehicle demand modeling based on 3d convolutional generative adversarial networks. *IEEE Transactions on Power Systems*, 37(2):1173–1183. DOI: 10.1109/TPWRS.2021.3100994.
- Kchaou-Boujelben, M. (2021). Charging station location problem: A comprehensive review on models and solution approaches. *Transportation Research Part C: Emerging Technologies*, 132:103376. DOI: 10.1016/j.trc.2021.103376.
- Lam, A. Y. S., Leung, Y.-W., and Chu, X. (2014). Electric vehicle charging station placement: Formulation, complexity, and solutions. *IEEE Transactions on Smart Grid*, 5(6):2846–2856. DOI: 10.1109/TSG.2014.2344684.
- Liimatainen, H., van Vliet, O., and Aplyn, D. (2019). The potential of electric trucks – an international commodity-level analysis. *Applied Energy*, 236:804–814. DOI: 10.1016/j.apenergy.2018.12.017.
- Lin, J., Zhou, W., and Wolfson, O. (2016). Electric vehicle routing problem. *Transportation research procedia*, 12:508–521. DOI: 10.1016/j.trpro.2016.02.007.
- Machado, C. A. S., Takiya, H., Yamamura, C. L. K., Quintanilha, J. A., and Berssaneti, F. T. (2020). Placement of infrastructure for urban electromobility: A sustainable approach. *Sustainability*, 12(16):6324. DOI: 10.3390/su12166324.
- Omohundro, S. M. (1989). Five balltree construction algorithms. *International Computer Science Institute*. Available at: [https://steveomohundro.com/wp-content/uploads/2009/03/omohundro89\\_five\\_balltree\\_construction\\_algorithms.pdf](https://steveomohundro.com/wp-content/uploads/2009/03/omohundro89_five_balltree_construction_algorithms.pdf).
- O’Connell, A., Pavlenko, N., Bieker, G., and Searle, S. (2023). A comparison of the life-cycle greenhouse gas emissions of european heavy-duty vehicles and fuels. *International Council on Clean Transportation: Washington, DC, USA*, pages 1–36. Available at: <https://theicct.org/wp-content/uploads/2023/02/lcaghg-emissions-hdv-fuels-europe-feb23.pdf>.
- Santos, G., Melos, G., Figueiredo, L., Silva, F., Silva, T., and Loureiro, A. (2024). Hexagonal p-median: Um modelo para alocação de pontos de recarga para caminhões elétricos. In *Anais do VIII Workshop de Computação Urbana*, pages 169–182, Porto Alegre, RS, Brasil. SBC. DOI: 10.5753/courb.2024.3278.
- Tamba, M., Krause, J., Weitzel, M., Ioan, R., Duboz, L., Grosso, M., and Vandyck, T. (2022). Economy-wide impacts of road transport electrification in the eu. *Technological forecasting and social change*, 182:121803. DOI: 10.1016/j.techfore.2022.121803.
- Tobler, W. R. (1970). A computer movie simulating urban growth in the detroit region. *Economic geography*, 46(sup1):234–240. DOI: 10.2307/143141.
- Viswanathan, V., Zehe, D., Ivanchev, J., Pelzer, D., Knoll, A., and Aydt, H. (2016). Simulation-assisted exploration of charging infrastructure requirements for electric vehicles in urban environments. *Journal of Computational Science*, 12:1–10. DOI: 10.1016/j.jocs.2015.10.012.
- Wu, J., Powell, S., Xu, Y., Rajagopal, R., and Gonzalez, M. C. (2024). Planning charging stations for 2050 to support flexible electric vehicle demand considering individual mobility patterns. *Cell Reports Sustainability*, 1(1). Available at: [https://www.cell.com/cell-reports-sustainability/fulltext/S2949-7906\(23\)00006-X?uuiid=uuid%3A7d704f4f-1af7-4044-9dd5-f4b06064680b](https://www.cell.com/cell-reports-sustainability/fulltext/S2949-7906(23)00006-X?uuiid=uuid%3A7d704f4f-1af7-4044-9dd5-f4b06064680b).
- Xiong, Y., An, B., and Kraus, S. (2021). Electric vehicle charging strategy study and the application on charging station placement. *Autonomous Agents and Multi-Agent Systems*, 35(1):1–19. DOI: 10.1007/s10458-020-09484-5.
- Xiong, Y., Gan, J., An, B., Miao, C., and Bazzan, A. L. (2017). Optimal electric vehicle fast charging station placement based on game theoretical framework. *IEEE Transactions on Intelligent Transportation Systems*, 19(8):2493–2504. DOI: 10.1109/TITS.2017.2754382.
- Zafar, U., Bayram, I. S., and Bayhan, S. (2021). A gis-based optimal facility location framework for fast electric vehicle charging stations. In *2021 IEEE 30th International Symposium on Industrial Electronics (ISIE)*, pages 1–5. IEEE. DOI: 10.1109/ISIE45552.2021.9576448.